# Recognition of Images Degraded by Gaussian Blur

Jan Flusser, Tomáš Suk(✉), Sajad Farokhi, and Cyril Höschl IV

Institute of Information Theory and Automation of the CAS,
Pod Vodárenskou věží 4, 182 08 Praha 8, Czech Republic
{flusser,suk,fsajad2,hoschl}@utia.cas.cz

**Abstract.** We introduce a new theory of invariants to Gaussian blur. The invariants are defined in Fourier spectral domain by means of projection operators and, equivalently, in the image domain by means of image moments. The application of these invariants is in blur-invariant image comparison and recognition. The behavior of the invariants is studied and compared with other methods in experiments on both artificial and real blurred and noisy images.

**Keywords:** Blurred image · Object recognition · Blur invariant comparison · Gaussian blur · Projection operators · Image moments · Moment invariants

## 1 Introduction

Image recognition/classification in general is an extremely broad area which apparently cannot be resolved by a single always-optimal method. This is why numerous specific formulations of the problem have appeared which consequently have resulted in many particular algorithms or classes of algorithms. Some of them have already become an established discipline of image analysis while some others are still undergoing initial development. One of the representatives of the latter group are methods for recognition of images which are degraded by a uniform Gaussian blur.

The mathematical formulation of the problem is well known in image processing. Capturing an ideal scene $f$ by an imaging device with the point-spread function (PSF) $h$, the observed image $g$ is a convolution of both

$$g(x, y) = (f * h)(x, y). \tag{1}$$

This linear space-invariant image formation model, even if it is very simple, is a reasonably accurate approximation of many imaging devices and acquisition scenarios. In this paper, we concentrate our attention to the case when the PSF is a Gaussian (with unknown parameters).

Gaussian blur appears whenever the acquisition was accomplished through a turbulent medium and the acquisition/exposure time is by far longer than


G. Azzopardi and N. Petkov (Eds.): CAIP 2015, Part I, LNCS 9256, pp. 88–99, 2015.
DOI: 10.1007/978-3-319-23192-1_8

the period of Brownian motion of the particles in the medium. Ground-based astronomical imaging through the atmosphere, taking pictures through a fog, fluorescence microscopy, and underwater imaging are three typical examples of such situation (in these cases, the blur may be coupled with a contrast decrease). Gaussian blur is also introduced into the images as the sensor blur which is due to a finite size of the sampling pulse; this effect is, however, mostly of low significance. Moreover, Gaussian kernel is often used as an approximation of some other blurs which are too complicated to work with them exactly. Gaussian blur is sometimes even introduced intentionally, for instance to suppress additive noise, to "soften" the image or before the image down-scaling and building the image pyramid. So, we can see there is actually a demand for having the tools designed particularly for processing Gaussian-blurred images.

Let us imagine a classification problem, when we need to classify a blurred image $g$ against a database of clear images. (The database typically consists of images acquired under good imaging conditions, so their blur can be considered much smaller than the blur of the query image or even negligible. In template matching, when the template has been extracted from the blurred image, the term "database" may refer to a single clear image of a scene in which the template should be located.) We have basically three options. The most time-expensive one is to generate all possible blurred versions of all templates (i.e. blurring with Gaussians the variances of which fill a reasonable, properly sampled interval) and incorporate them into the database. This brute-force approach is not practically feasible.

Another approach relies on the solution of the inverse problem, when the blur is removed from the input image and the deblurred image is then classified by any standard technique. This process contains semi-blind image deconvolution (the term "semi-blind" is used because we know the parametric form of the kernel but its parameter(s) are unknown), which is in the case of a Gaussian kernel an unstable, ill-posed problem. Unlike motion blur and out-of-focus blur, Gaussian blur does not introduce any zero patterns into the spectrum of the image, which are in the other cases employed for parameter estimation. Only few semi-blind deconvolution methods w.r.t. Gaussian blur have been published. They first try to estimate the size (variance) of the blur and then to perform a non-blind deconvolution [6] [1], [2], [11], [10]. All these methods are sensitive to variance overestimation and relatively time-consuming.

The third and the most promising approach is based on the idea that for blur-insensitive recognition we do not need to restore the query image, we only need its representation which might be lossy but robust w.r.t. the Gaussian blur. Such a representation should describe those features of the image, which are not affected by the degradation. Since the classification is mostly performed by minimum distance rule in some (usually Euclidean) feature space, the task of finding a proper representation is always coupled with the task of defining a blur-robust distance measure. Technically speaking, we are looking for a distance measure $d$ between two images such that

$$d(f_1, f_2) = d(f_1 * h, f_2) \tag{2}$$

for any Gaussian kernel $h$. Instead of an explicit definition of blur-invariant distance $d$, we may look for a blur-invariant feature descriptor $I$ such that

$$I(f) = I(f * h) \tag{3}$$

and then use one of standard vector metrics for evaluating the distance between $I(f)$ and the same representation of the database templates.

Several authors have tried to derive invariants (3) w.r.t. Gaussian blur. Tianxu [7] realized without a deeper analysis that the complex moments of the image, one index of which is zero, are invariant to Gaussian blur. Xiao [9] seemingly derived invariants to Gaussian blur but he did not employ the parametric Gaussian form explicitly. He only used the circular symmetry property which lead to an incomplete invariant system. Gopalan et al. [5] derived another invariant set without assuming the knowledge of the parametric shape of the kernel but imposed a limitation of its support size. Flusser et al. derived blur invariants for centrosymmetric kernels [3] and later for arbitrary $N$-fold symmetric kernels [4]. All the methods mentioned above do not use the parametric form of the PSF at all. Although they can be applied to Gaussian blur, too, because the Gaussian kernel is a particular case of symmetric kernels, they do not reach the maximum discrimination power. Specific invariants to Gaussian blur providing an optimal discriminabilty cannot be obtained as a special case of these methods (even if the idea of projection operators we employ in this paper is similar to that we proposed in [4]).

The most promising approach so far was proposed by Zhang et al. [13], [12], who employed Gaussian parametric form to derive a blur-invariant similarity measure between two images of the type (2), without deriving blur invariants explicitly. The method looks elegant and the authors reported a good performance. However, a serious weakness of the Zhang's method is its high complexity and sensitivity to noise in the images to be compared, as will be demonstrated in the experimental part of this paper.

## 2 Gaussian Blur Invariants in the Spectral Domain

In this section we present an approach which is based on the *invariant descriptors* of the type (3). The basic conceptual difference from the Zhang's method is that these invariants are defined for a single image, while the Zhang's distance always requires a pair of images. So, we can calculate the invariant representations of the templates only once and store them in the database, which leads to much faster recognition.

### 2.1 Projection Operators in 1D

The new invariants are based on the projection of the image onto a space of unnormalized Gaussian functions, which preserves the image moments of the zero, the first, and the second orders. The separability of the 2D Gaussian function allows us to create a 1D theory (which is more transparent and easy to explain) first and then to generalize it to the 2D case.

Let us consider a 1D "image" $f$ with a finite non-zero integral and a finite second-order central moment. The projection operator $P_G$ is defined as

$$P_G(f)(x) = m_0 G_s(x), \tag{4}$$

where

$$G_s(x) = \frac{1}{\sqrt{2\pi}\sigma} e^{-\frac{x^2}{2s^2}},$$

$$s^2 = m_2/m_0$$

and

$$m_p = \int (x-c)^p f(x)dx \tag{5}$$

is the $p$-th central moment of $f$ (with $c$ being the centroid of $f$). Hence, $P_G$ assigns each $f$ to a multiple of a centralized Gaussian such that the central moments up to the second order of $f$ and $P_G(f)$ are the same. In other words, $P_G(f)$ is the "closest" unnormalized Gaussian to $f$ in terms of the moment values. In this sense, $P_G$ can be considered a projector onto the set of all unnormalized Gaussian functions. In particular, $P_G(G_\sigma) = G_\sigma$. An important property of $P_G$, which will be later used for construction of the invariants, is its relationship to a convolution with a Gaussian kernel

$$P_G(g)(x) \equiv P_G(f * G_\sigma)(x) = m_0 G_{\sqrt{(s^2+\sigma^2)}}(x) \equiv \frac{m_0}{\sqrt{2\pi(s^2+\sigma^2)}}\, e^{-\frac{x^2}{2(s^2+\sigma^2)}}.$$

Finally, we show how the operator $P_G$ behaves under the Fourier transform. Since the Fourier transform of a Gaussian $G_\sigma$ is an (unnormalized) Gaussian $G_{1/\sigma}$

$$\mathcal{F}(G_\sigma)(u) = e^{-2\pi^2\sigma^2u^2},$$

we have

$$\mathcal{F}(P_G(f))(u) = \mathcal{F}(m_0 G_s)(u) = m_0 e^{-2\pi^2 s^2 u^2}$$

and

$$\mathcal{F}(P_G(g))(u) \equiv \mathcal{F}P_G(f*G_\sigma)(u) = m_0 e^{-2\pi^2(s^2+\sigma^2)u^2} = \mathcal{F}(P_G(f))(u)\cdot\mathcal{F}(G_\sigma)(u).$$

### 2.2 1D Gaussian Blur Invariants in the Fourier Domain

Now we can formulate the central theorem of this paper.

**Theorem 1.** *Let $f$ be an image function. Then*

$$I_G(f)(u) = \frac{\mathcal{F}(f)(u)}{\mathcal{F}(P_G(f))(u)}$$

*is an invariant to Gaussian blur, i.e. $I_G(f) = I_G(f * G_\sigma)$ for any blur parameter $\sigma$.*

The proof follows immediately from the assertions introduced in the previous section. Note that $I_G$ is invariant also to the contrast stretching, $I_G(f) = I_G(af)$.

$I_G(f)$ can be viewed as a Fourier transform of the *primordial image*

$$f_r = \mathcal{F}^{-1}(I_G(f)).$$

However, $f_r$ is not an image in a common sense because the existence of $\mathcal{F}^{-1}(I_G(f))$ is not generally guaranteed and even if $f_r$ exists, it may contain negative values.

This is a kind of normalization w.r.t. Gaussian blurring of unknown extent. The primordial image plays the role of a canonical form of $f$, which actually is its "maximally deconvolved" non-Gaussian part.

The operator $I_G$ decomposes the image space into classes of equivalence. Fortunately, this decomposition is exactly the same as that one induced by the following relation: two functions $f_1$ and $f_2$ are equivalent if and only if there exists $\sigma \geq 0$ such that $f_1 = f_2 * aG_\sigma$ or $f_2 = f_1 * aG_\sigma$. This is an important observation, saying that $I_G(f)$ is a *complete* description of $f$ up to a convolution with a Gaussian and a multiplicative contrast change. In other words, $I_G(f)$ defines an *orbit*[1] of images equivalent with $f$. Thanks to the completeness, $I_G$ discriminates between the images from different orbits but obviously cannot discriminate inside an orbit. In particular, $I_G$ cannot discriminate between two Gaussians since all Gaussians lie on the orbit the root of which is the delta function.

### 2.3 1D Gaussian Blur Invariants in the Image Domain

In principle, we can use directly $I_G(f)$ as the invariant feature vector of the same size as $f$ but working in the Fourier domain brings two practical difficulties. Since $I_G(f)$ is a ratio, we possibly divide by very small numbers which requires an appropriate numerical treatment. Moreover, high frequencies of $I_G(f)$ use to be sensitive to noise. This can be overcome by suppressing them by a low-pass filter, but this procedure requires additional time and introduces a user-defined parameter which should be set up with respect to the particular noise level. That is why in most cases we prefer to work directly in the image domain, where invariants equivalent to $I_G(f)$ can be constructed.

To obtain the link between the Fourier and image domains, we use a Taylor expansion of the harmonic functions and a term-wise integration

$$\mathcal{F}(f)(u) \equiv \int_{-\infty}^{\infty} f(x) \cdot e^{-2\pi i u x} dx = \sum_{k=0}^{\infty} \frac{(-2\pi i)^k}{k!} m_k u^k. \tag{6}$$

The above formula tells us that the moments of the image are Taylor coefficients (up to a constant factor) of its Fourier transform. Analogous formula for $\mathcal{F}(P_G(f))$ is

$$\mathcal{F}(P_G(f))(u) = m_0 \sum_{k=0}^{\infty} \frac{(-2\pi^2)^k}{k!} \left(\frac{m_2}{m_0}\right)^k u^{2k}. \tag{7}$$

[1] The term "orbit" was introduced by Zhang in [12] in this context.

If the Taylor expansion of $I_G(f)$ is

$$I_G(f)(u) = \sum_{k=0}^{\infty} \frac{(-2\pi i)^k}{k!} a_k u^k, \tag{8}$$

where $a_k$ are the moments of the primordial image, we can rewrite Theorem 1 as

$$\sum_{k=0}^{\infty} \frac{(-2\pi i)^k}{k!} m_k u^k = m_0 \sum_{k=0}^{\infty} \frac{(-2\pi^2)^k}{k!} \left(\frac{m_2}{m_0}\right)^k u^{2k} \cdot \sum_{k=0}^{\infty} \frac{(-2\pi i)^k}{k!} a_k u^k.$$

Comparing the terms with the same power of $u$ we obtain, after some manipulation, the recursive expression for each $a_p$

$$a_p = \frac{m_p}{m_0} - \sum_{\substack{k=2 \\ k \text{ even}}}^{p} (k-1)!! \cdot \binom{p}{k} \left(\frac{m_2}{m_0}\right)^{k/2} a_{p-k}. \tag{9}$$

The symbol $k!!$ means a double factorial, $k!! = 1 \cdot 3 \cdot 5 \cdots k$ for odd $k$. Since the primordial image itself (more precisely, its Fourier transform) was proven to be blur invariant, each its moment must be also a blur invariant. If we restrict ourselves to a brightness-preserving blurring, then $m_0$ itself is an invariant and we obtain from (9) the simplified final form of Gaussian blur invariants

$$B(p) \equiv m_0 a_p = m_p - \sum_{\substack{k=2 \\ k \text{ even}}}^{p} (k-1)!! \cdot \binom{p}{k} \left(\frac{m_2}{m_0}\right)^{k/2} B(p-k). \tag{10}$$

As we already said, $B(p)$ is actually a $p$-th moment of the primordial image of $f$. Regardless of $f$, $B(1) = 0$ because we work with central moments because the second-order moment was used to eliminate the unknown blur parameter $\sigma$. Hence, $B(1)$ and $B(2)$ should not be used in the feature vector since they do not carry any information.

In addition to higher robustness, using the image-domain features (10) is also faster than using $I_G$. In practice, we do not need a complete representation of the images in question. Usually a few invariants provide a sufficient discrimination power, so we use the $B(p)$'s up to the certain order $Q$ only. This $Q$ is a user-defined parameter the determination of which should be based on a discrimination analysis of the database images. The choice of $Q$ is always a compromise between the discriminative power and the complexity of the method.

### 2.4 Gaussian Blur Invariants in Two Dimensions

Now let us assume the image domain is a subset of $R^2$. The centralized 2-D Gaussian function has the form

$$G_C(\mathbf{x}) = \frac{1}{2\pi\sqrt{|C|}} \exp\left(-\frac{1}{2}\mathbf{x}C^{-1}\mathbf{x}'\right), \tag{11}$$

where $\mathbf{x} \equiv (x_1, x_2)$ and $C$ is the covariance matrix which determines the shape of the Gaussian. Provided that the covariance matrix of the blur kernel is diagonal, we define the projection operator as

$$P_G(f)(\mathbf{x}) = m_{00} G_\Sigma(\mathbf{x}), \tag{12}$$

where

$$\Sigma = \mathrm{diag}(m_{20}/m_{00}, m_{02}/m_{00}).$$

Then

$$I_G(f)(\mathbf{u}) = \frac{\mathcal{F}(f)(\mathbf{u})}{\mathcal{F}(P_G(f))(\mathbf{u})}$$

is a blur invariant and after applying the Taylor expansion, we end up with the following moment invariants analogous to (10)

$$B(p,q) = m_{pq} - \sum_{\substack{k+j=2 \\ k,j \text{ even}}}^{p,q} (k-1)!! \cdot (j-1)!! \cdot \binom{p}{k} \binom{q}{j} \left(\frac{m_{20}}{m_{00}}\right)^{k/2} \left(\frac{m_{02}}{m_{00}}\right)^{j/2} B(p-k, q-j). \tag{13}$$

Note that we are not limited to circularly symmetric Gaussian blur kernels but we allow different extent of the blur in $x_1$ and $x_2$ directions. This may be useful when the horizontal and vertical resolutions of the sensor differ from each other.

## 3 Experiments and a Comparison to the Zhang's Method

The aim of this section is not only to demonstrate the performance of the proposed method but also to compare it with the method by Zhang et al. [12]. To make the comparison as fair as possible, we asked the authors of [12] for providing all necessary codes. Then we implemented our method using the same version of Matlab (R2013a) and always run both on the same computer (Dell Notebook, VOSTRO 1510, Intel, Core2 Duo CPU, 4GB RAM, Windows 8, 32-bit) and on the same test images. Since the Zhang's method can compare only images of the same size, we kept this condition in all experiments.

### 3.1 Blur Invariance Property

As we expected, both methods actually exhibit high invariance w.r.t. a "perfect" (i.e. computer generated) Gaussian blur (see Table 1). We changed the blur parameter $\sigma$ from 0 to 7 and calculated both the invariant distance (ID) and the Zhang's distance (ZD) between the blurred image and the original. Both are reasonably small although not zero. The non-zero values appear because the sampled Gaussian does not fulfil exactly the assumption. For comparison, we also calculated the distances between several *different* originals of the same size, which is by many orders higher.

**Table 1.** The values of ZD and ID in case of simulated Gaussian blur

| Filter size | Sigma | ZD | ID |
|---|---|---|---|
| 1 | 0 | 0 | 0 |
| 9 | 1 | 0.112 | 2e-19 |
| 17 | 2 | 0.005 | 1e-19 |
| 25 | 3 | 0.009 | 3e-19 |
| 33 | 4 | 0.012 | 4e-19 |
| 41 | 5 | 0.014 | 6e-19 |
| 49 | 6 | 0.016 | 2e-19 |
| 57 | 7 | 0.017 | 2e-19 |

(a) (b) (c)

**Fig. 1.** Test image "windmills": (a) original, (b) blurred, (c) blurred with noise.

### 3.2 Matching of Blurred Templates - Simulated Blur

In this experiment we tested the performance in the template matching, which is a particular classification problem we often face in practice. Assuming that we have a large clear image of a scene and a blurred template, the task is to localize this template in the clear image. For non-blurred templates, cross-correlation has been traditionally used to resolve this task. For blurred templates, we again tested both ID and ZD and for a comparison we included also the cross-correlation. Since the testing of each possible template location is very time consuming, we used all three methods in a hierarchical coarse-to-fine implementation. On the coarse level, we shifted the template by the step of 4 pixels in both directions. On the fine level, we searched a $9 \times 9$ neighborhood of the "best" location found in the coarse level. Provided that the horizontal and vertical localization errors are independent and both have the same normal distribution, the absolute localization error has a Rayleigh distribution. We estimated the mean values and standard deviations of the localization error of all three methods, which illustrates the accuracy. Since these parameters might be influenced by few big errors, we also calculated the number of "correct hits", which may serve as another accuracy measure. We marked the position of the template found by the algorithm as a hit, if its localization error was less or equal to one pixel in each direction.

Note that in template matching, when the blurred templates have been extracted from a large scene, we always face a boundary effect. This means there is a strip along the template boundary where the convolution model is not valid (even if the blur has been introduced artificially) because the pixels laying outside the template also contribute to the intensity values inside this strip due to the blurring kernel. The boundary effect is the main source of errors in a noise-free case.

We used a simulated blur. We took a clear image of the size $256 \times 256$, blurred it by a $13 \times 13$ Gaussian of $\sigma = 2$ and randomly selected 30 templates of the size $32 \times 32$. These templates were searched in the clear image. We used the invariants up to the order six. The results of the matching in terms of the accuracy and computational time are summarized in Table 2. We can see that the accuracy of both ID and ZD are excellent, so both methods are stable w.r.t. the boundary effect. The ZD yields even better localization error than ID because it uses a complete information about the template while the invariants work with highly compressed information. On the other hand, ID is more than 20 times faster than ZD. The cross-correlation was much faster than ID but its accuracy was very low because of the blurring. The time measurement for one template includes a complete "scan" of the scene including invariant and distance calculation for each tested position and search for the minimum distance. Overheads (reading of the images, generating blur kernel, blurring the image, template selection, etc.) are common for all methods and were not included into the measurement.

**Table 2.** Matching of blurred templates

| Methods | Mean error | Std | Mean time complexity(s) | Correct hits |
|---|---|---|---|---|
| Cross-correlation | 42.53 | 22.22 | 1.29 | 23 |
| ZD | 0.16 | 0.08 | 831.54 | 30 |
| ID | 0.39 | 0.20 | 34.55 | 30 |

**Table 3.** Matching of blurred and noisy templates

| Methods | Mean error | Std | Mean time complexity(s) | Correct hits |
|---|---|---|---|---|
| Cross-correlation | 41.24 | 21.55 | 1.31 | 20 |
| ZD | 43.99 | 22.98 | 825.11 | 15 |
| ID | 0.90 | 0.47 | 33.11 | 28 |

Then we repeated the same experiment with the same setting and with the same templates but we added a Gaussian white noise of SNR = 10 dB into the blurred image (see Fig. 1). As can be seen from Table 3, the results changed dramatically. The ID still provides 28 correct hits and the mean error less than one, while the ZD was even worse than the cross-correlation. The invariant method is robust because the moments are defined as integrals, which basically "averages" the noise and decreases its impact on the feature values. On the other hand,

the Zhang distance is very sensitive. This is because in this method the image blur level is estimated by measuring the energy in the high-pass band. The noise dominates the image on high frequencies and contributes a lot to this measure. Hence, the blurred image with a noise may often be considered "sharper" than the clear image, which leads to a wrong estimate of the blur level and to incorrect distance calculation. The time complexity is basically the same as in the first experiment.

### 3.3 Matching of Blurred Templates - Real Blur

We repeated the same experiment with a real blur. We employed two images of the spot in the solar photosphere taken by a telescope with a CCD camera in a visible spectral band (venue: Observatory Ondřejov, Czech Republic; wavelength: $\lambda \doteq 590$ nm). Since the time interval between the two acquisitions was only a few minutes, the scene can be considered still and the images are almost perfectly registered. As the atmospheric conditions changed between the acquisitions, the first image is relatively sharp while the other one is noticeably blurred by the atmospheric turbulence (see Fig. 2). The blur kernel is believed to be approximately Gaussian (an experimental validation of this assumption can be found for instance in [8]). Mild additive noise is present in both images. By the same algorithm as in the previous case, we matched 20 randomly chosen templates extracted from the blurred image against the "clear" image. The size of the images was $175 \times 175$, the template size was $32 \times 32$, and the maximum order of the invariants used was six. As one can see from Table 4, the results are consistent with those we achieved on simulated blurring: ZD performs insignificantly better localization than ID on the expense of the time complexity.

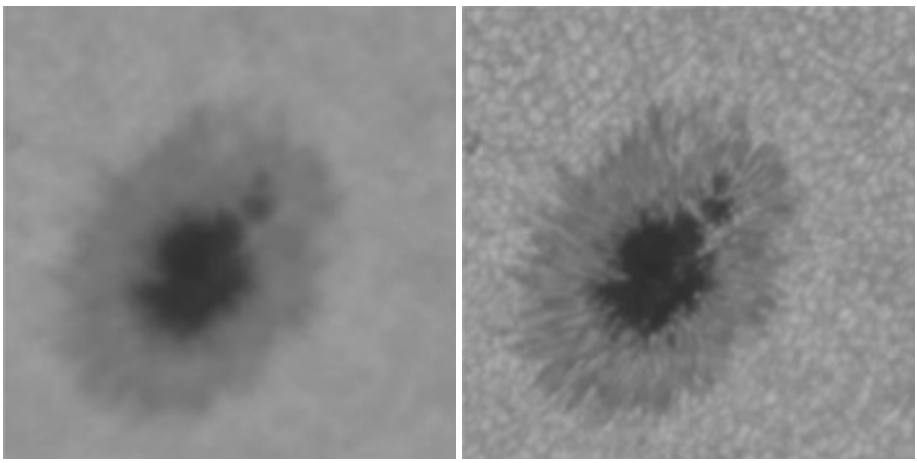

(a) (b)

**Fig. 2.** Detail of solar photosphere (a) with higher blur, (b) with lower blur.

**Table 4.** Template matching in astronomical images

| Methods | Mean error | Std | Mean time complexity(s) | Correct hits |
|---|---|---|---|---|
| Cross-correlation | 11.83 | 6.18 | 0.47 | 16 |
| ZD | 0.74 | 0.38 | 329.72 | 20 |
| ID | 0.81 | 0.42 | 15.74 | 20 |

## 4 Conclusion

We proposed new invariants w.r.t. Gaussian blur, both in frequency and image domains. We showed the performance of the new method in matching of blurred and noisy templates. Comparing to the Zhang's method [12], which has been the only Gaussian-blur invariant metric, the proposed method is significantly faster and more robust to additive noise.

**Acknowledgments.** The authors express their gratitude to the Czech Science Foundation for financial support of this work under the grant No. GA15-16928S. Thanks to Observatory Ondřejov for their help with accessing the images of the solar photosphere.

## References

1. Carasso, A.S.: The APEX method in image sharpening and the use of low exponent Lévy stable laws. SIAM Journal on Applied Mathematics **63**(2), 593–618 (2003)
2. Elder, J.H., Zucker, S.W.: Local scale control for edge detection and blur estimation. IEEE Transactions on Pattern Analysis and Machine Intelligence **20**(7), 699–716 (1998)
3. Flusser, J., Suk, T.: Degraded image analysis: An invariant approach. IEEE Transactions on Pattern Analysis and Machine Intelligence **20**(6), 590–603 (1998)
4. Flusser, J., Suk, T., Boldyš, J., Zitová, B.: Projection operators and moment invariants to image blurring. IEEE Transactions on Pattern Analysis and Machine Intelligence **37**(4), 786–802 (2015)
5. Gopalan, R., Taheri, S., Turaga, P., Chellappa, R.: A blur-robust descriptor with applications to face recognition. IEEE Transactions on Pattern Analysis and Machine Intelligence **34**(6), 1220–1226 (2012)
6. Honarvar Shakibaei, B., Flusser, J.: Image deconvolution in moment domain. In: Papakostas, G.A. (ed.) Moments and Moment Invariants - Theory and Applications Gate to Computer Science and Research, vol. 1, pp. 111–125. Science Gate Publishing (2014)
7. Liu, J., Zhang, T.: Recognition of the blurred image by complex moment invariants. Pattern Recognition Letters **26**(8), 1128–1138 (2005)
8. Šroubek, F., Flusser, J.: Multichannel blind iterative image restoration. IEEE Transactions on Image Processing **12**(9), 1094–1106 (2003)
9. Xiao, B., Ma, J.F., Cui, J.T.: Combined blur, translation, scale and rotation invariant image recognition by Radon and pseudo-Fourier-Mellin transforms. Pattern Recognition **45**, 314–321 (2012)

10. Xue, F., Blu, T.: A novel SURE-based criterion for parametric PSF estimation. IEEE Transactions on Image Processing **24**(2), 595–607 (2015)
11. Zhang, W., Cham, W.K.: Single-image refocusing and defocusing. IEEE Transactions on Image Processing **21**(2), 873–882 (2012)
12. Zhang, Z., Klassen, E., Srivastava, A.: Gaussian blurring-invariant comparison of signals and images. IEEE Transactions on Image Processing **22**(8), 3145–3157 (2013)
13. Zhang, Z., Klassen, E., Srivastava, A., Turaga, P., Chellappa, R.: Blurring-invariant riemannian metrics for comparing signals and images. In: IEEE International Conference on Computer Vision, ICCV 2011, pp. 1770–1775 (2011)